Title	Low-pressure, high-temperature thermal bonding of polymeric microfluidic devices and their applications for electrophoretic separation
Author(s)	Sun, Yi; Kwok, Yien Chian; Nguyen, Nam-Trung
Citation	Sun, Y., Kwok, Y. C., & Nguyen, N. T. (2006). Low-pressure, high-temperature thermal bonding of polymeric microfluidic devices and their applications for electrophoretic separation. Journal of Micromechanics and Microengineering, 16(8).
Date	2006
URL	http://hdl.handle.net/10220/7818
Rights	© 2006 IOP Publishing Ltd. This is the author created version of a work that has been peer reviewed and accepted for publication by Journal of micromechanics and microengineering, IOP Publishing Ltd. It incorporates referee's comments but changes resulting from the publishing process, such as copyediting, structural formatting, may not be reflected in this document. The published version is available at: [DOI: http://dx.doi.org/10.1088/0960-1317/16/8/033].

Low-pressure, high-temperature thermal bonding of polymeric microfluidic devices and their applications for electrophoretic separation

***Yi Sun*[1], *Yien Chian Kwok*[1], *Nam-Trung Nguyen*[2,] ***

[1]*National Institute of Education, 1 Nanyang Walk, 637616, Singapore*

[2]*School of Mechanical and Aerospace Engineering, Nanyang Technological University, 50 Nanyang Avenue, 639798, Singapore*

E-mail: mntnguyen@ntu.edu.sg

Abstract

A new method for thermally bonding poly(methyl methacrylate) (**PMMA**) substrates has been demonstrated. **PMMA** substrates are first engraved by CO_2-laser micromachining to form microchannels. Both channel width and depth can be adjusted by varying the laser power and scanning speed. Channel depths from 50 μm to 1500 μm and widths from 150 μm to 400 μm are attained. CO_2 laser is also used for drilling and dicing of the **PMMA** parts. Considering the thermal properties of **PMMA**, a novel thermal bonding process with high temperature and low bonding pressure has been developed for assembling **PMMA** sheets. A high bonding strength of 2.15 MPa is achieved. Subsequent inspection of the cross sections of several microdevices reveals that the dimensions of the channels are well preserved during the bonding process. Electroosmotic mobility of the ablated channel is measured to be 2.47×10^{-4} cm^2 V^{-1} s^{-1}.The functionality of these thermally bonded microfluidic substrates is demonstrated by performing rapid and high-resolution electrophoretic separations of a mixture of fluorescein and carboxyfluorescein as well as double-stranded DNA ladders ($\phi X174$-*Hae III* dsDNA digest). The performance of the CO_2-laser ablated and thermally bonded **PMMA** devices compares favorably to those fabricated by other professional means.

1 Introduction

Poly(methyl methacrylate) (**PMMA**) has been used as a basic substrate material for the fabrication of microfluidic devices due to its high mechanical stability [1], good chemical properties and excellent optical clarity [2]. The manufacturing process of **PMMA** microchips has received intensive attention. Several fabrication methods such as hot embossing [3], injection molding [4], LIGA (German acronym for x-ray lithography electro deposition and molding) [1, 5] and excimer laser (ultra violet laser) ablation [6] have been studied. For replication methods such as hot embossing and injection molding, the costly and time-consuming mold fabrication process hampers the rapid turnaround of new design although the technology is intrinsically suitable for mass production. The implementations of x-ray lithography and excimer laser ablation are expensive because of the high cost of the x-ray and excimer laser system and the corresponding masks. Recently, the cheaper CO_2 laser has been used to create microchips in **PMMA** [7, 8]. This technique has been proven to be rapid and effective for fabricating microfluidic devices especially for scientific trials and small-scale production.

One of the key challenges in creating any microfluidic devices is to realize an effective seal by affixing a cover plate to a substrate containing microfabricated channels. Several methods for bonding **PMMA** substrates have been demonstrated, including thermal bonding in a convectional oven [9], in boiling water [10] or with heated weights [11], microwave welding [12], adhesive printing [1], solvent bonding [13] and thermal lamination [14]. At the most basic level, gluing substrates together affords an adequate seal. However, this approach is often limited by the high risks of channel blockages. Thermal lamination with a polyethylene terephthalate (PET)/polyethylene (PE) film is a more common solution to the bonding problem. The adhesive tape offers a better controllability of the bonding process. Lamination can be achieved using standard industrial lamination apparatus at temperatures around 100 ˚C. However, when using thermal lamination, the channel is defined by different materials and the resultant inhomogeneities in zeta potential can cause band broadening [15, 16]. Hence, direct thermal bonding approaches are especially desirable as they

allow formation of enclosed microchannels with uniform surfaces composed entirely of the same polymeric material. The technique was studied by Shadpour *et al* [2], Alonso-Amigo and Adams [17] or Liu *et al* [18]. In their works, the bonding temperatures were kept just over glass transition temperature (107 °C for **PMMA** [2, 17] and 134 °C for polycarbonate (PC) [18]), and relatively high bonding pressures were applied. However, high bonding pressure may induce global and localized geometric deformation of the substrates or leave an interfacial layer with significant thickness variation. To guarantee the structural integrity of the polymeric substrates, thermal bonding with lower pressure is desired.

In this paper, we demonstrate a novel thermal bonding technique for **PMMA** substrates. The microchannels are engraved by CO_2-laser micromachining which is also used to dice **PMMA** sheets and drill access holes. The microchannel width and depth are controlled by varying the laser power and scanning speed of the laser beam. The new thermal bonding method is proposed according to the thermal properties of **PMMA**. In contrast to the previous works, our approach employs elevated temperature (165°C for **PMMA**) and low pressure during the bonding process. The elevated temperature leads to high bonding strength and the low bonding pressure assures good structural integrities. High quality bonding has been achieved with no signs of deformation and interfacial layer. Bonding strength and electroosmotic mobility of the microfabricated devices are measured. Application of the microchips are investigated by performing capillary electrophoretic (CE) separation of mixture of fluorescein and carboxyfluorescein, and $\phi X174$-*Hae III* dsDNA digest ladder.

2 Experimental section

2.1 Microfabrication

The microfluidic pattern was designed using CorelDraw 10 (Corel Co., Canada). The pattern was then sent to a laser scriber for direct micromachining on **PMMA** substrate. The commercial CO_2

laser scriber (Universal M-300 Laser Platform, Universal Laser Systems Inc., Arizona, USA) was used to engrave the **PMMA** substrate. The CO_2 laser has a wavelength of 10.6 μm and its maximum power is 25 W. A focused laser beam can scan over a two-dimensional area by the combined motion of *X* and *Y* stages. The maximal speed of the laser beam motion is 640 mm s^{-1}. The dimension of microchannels was achieved by controlling laser power and scanning speed. Access holes were also drilled by the CO_2 laser to allow fluid access to the microchannels. Microchannel widths and depths were measured using a scanning electron microscope (SEM) (N3500S, Hitachi Science Systems Ltd., Japan).

To form the microfluidic device, the trench was sealed by the novel thermal bonding technique. The experimental implementation of this bonding technique is simple. A hot plate was used for the temperature control. The **PMMA** sheets were placed between the hotplate and an upper aluminium plate. Bonding pressure could be adjusted by putting weights on top of the upper plate and it was kept at around 20 kPa or less. To achieve a better surface flatness of the **PMMA** layers, one polished silicon wafer was placed between the hot plate and the **PMMA** sheets, and another wafer was put between the **PMMA** sheets and the upper aluminium plate. Prior to the bonding process, the **PMMA** parts were carefully cleaned by rinsing in ethanol and then deionized (DI) water. The temperature regime of the bonding process is shown in table 1. The **PMMA** sheets were heated to 165 °C in 10 min, and then they were bonded at 165 °C for 30 min. Next, the bonded stack was cooled down to 80 °C in 20 min and annealed at this temperature for another 30 min to relieve stress. Finally, the bonded device was cooled to room temperature. The whole bonding process took about 2 h, which is considerably shorter than the thermal bonding using conventional oven [19], where the bonding process took at least 3 h.

Figure 1 shows the schematic diagram of the **PMMA** micro CE chip. The simple cross geometry is designed for sample injection and separation. The microchannel defined by points A and D was the separation microchannel and that defined by points B and C was the injection microchannel. At the end of each microchannel, there were reservoirs for sample, buffer, or waste.

These reservoirs also provided access of the electrodes for high-voltage input. The microchannels were 100 μm wide and 30 μm deep. The lengths of separation and injection microchannels were 8 cm and 2 cm, respectively.

2.2 Bonding strength characterization

The tensile strength of the bond between two **PMMA** substrates was determined using an Instron 3369 tensile tester (Instron, Toronto, ON, CA). Two strips of **PMMA** (75 mm × 25 mm × 1 mm) were overlapped (3 cm^2) and then thermally bonded to one another. The test specimen was clamped into the tensile tester with grips set 80 mm apart, and pulled away from each other at a rate of 1mm min^{-1}. The force at which the bonded **PMMA** failed was measured. The shear bond strength of the specimen was calculated using equation (1):

$$\text{Bond strength} = \frac{\text{Break\_force}}{\text{Bonding\_surface\_area}}. \quad (1)$$

2.3. Electroosmotic flow (EOF) measurements

The electroosmotic mobility (μ_{eo}) of the fabricated **PMMA** microchip was measured by the current monitoring technique [20]. A straight channel with a cross section of 100 μm × 30 μm and a length of 8 cm was used for the measurement. Initially, both reservoirs and the microchannel were filled with 18 mM 2-(4-morpholino)ethanesulfonic acid (MES, pH 7.2) (Sigma, MO, USA) and the fluid was run with an electric field of 375 V cm^{-1} from the anode to cathode. After 10 min, the anodic reservoir was emptied and refilled with 20 mM MES. The electric field was applied again and the current passing through the channel was monitored continuously by an amperometric detector. The EOF velocity was determined according to the equation: $v_{EOF} = L/t$, where L is the channel length and t is the time required for the higher-concentration buffer to fill the microchannel. The EOF mobility was given by the ratio of v_{EOF} to the applied electric field strength E.

2.4. Detection apparatus

Microchip electrophoresis with laser induced fluorescence (LIF) detection was performed on an inverted confocal microscope (TCS SP2, Leica Microsystems AG, Germany). The output radiation (488 nm) from an Argon ion laser first passed through a programmable acousto optical tunable filter (AOTF). The AOTF was configured as a 488 nm band pass filter. The laser beam was then reflected by an electronically controlled 500 nm acousto optical beam splitter (AOBS) and into a 25× long field objective (0.4 NA). The laser beam was focused onto the separation channel 3.5 cm from the intersection point, resulting in an effective separation length of 3.5 cm. Subsequently, fluorescence was collected by the same objective and transmitted back through the AOBS. The emission beam was then focused through a pinhole of 340 μm and passed through a programmable 525 nm spectrophotometer prism (SP) barrier filter. The emission beam was finally detected by a highly sensitive side-window photomultiplier tube (PMT) with a gain of 800 V/V. Confocal imaging of the detection volume of the microchannel was accomplished by beam scanning with a proprietary K scanner. Data were collected and processed by Leica confocal software (LCS) program.

2.5. Microchip electrophoretic separation

For free solution electrophoresis, 0.1 × TBE was used as running buffer. Fluorescein (Invitrogen Co., California, USA) and 5(6)-Carboxyfluorescein (Sigma Chemical Co., Missouri, USA) were dissolved in 0.1×TBE as sample solution and the final concentrations were 100 nM and 200 nM, respectively. All solutions were prepared with deionized (DI) water and filtered through a 0.45 μm filter (Nalgene^{TM}, Sybron Co., New York, USA) before use. Due to the multiple negative charges associated with the two dyes, their electrophoretic mobilities were found to be greater than the electroosmotic flow generated by the **PMMA** device, causing their net mobility from the cathodic to the anodic reservoir. Hence, during the free solution electrophoresis, reverse polarity was used. The voltages for the four reservoirs were generated by a commercial 4-channel kilovolt power supply

(MCP 468, CE resources Pte Ltd, Singapore). The potentials and the switching protocol were controlled by a MCP 468 program operated on an IBM compatible PC. The voltage program for sample injection and separation are listed in table 2.

The DNA electrophoretic separation was also run in reverse polarity. The separation running buffer consists of 3.5% Hydroxypropylcellulose (HPC, 100 000 MW, Sigma, MO, USA) in 80 mM MES/40 mM tris(hydroxymethylamino) methane (TRIS) (Sigma, MO, USA). Intercalating dye YOPRO-1 (Invitrogen, USA) was added to a concentration of 10 μM. The DNA sizing ladder, $\phi X174$-*Hae III* dsDNA digest (Invitrogen, USA) was dissolved in autoclaved DI water to a final concentration of 5 μg mL^{-1}. DNA molecules were stained with the intercalating dye during the migration in microchannels. For DNA loading, an electric field of 350 V cm^{-1} was applied between the sample reservoir and the sample waste reservoir for 30 s, while both the buffer and the buffer waste reservoirs were allowed to float. Following sample injection, electric field was then switched to the separation channel and subsequent separation occurred. An electric field strength of 300 V cm^{-1} was applied across the buffer and the buffer waste reservoirs. To prevent leakage of extraneous DNA into the separation channel, a pull back voltage of 0.5 kV was applied to sample inlet and waste reservoirs to create a field strength that was approximately 10% of the total field strength in the separation channel.

3 Results and discussions

3.1 Micromachining with CO_2-laser

The CO_2 laser has a relatively long characteristic wavelength of 10.6 μm and emits radiation continuously. It is very versatile and available with a wide range of output powers and at a reasonable cost. However, the CO_2 laser is not good at generating smaller features due to its long operating wavelength, and channels less than 100 μm cannot be effectively fabricated. Wherever the focused laser beam meets the substrate surface, the temperature of the irradiated spot will raise so rapidly that

the material will first melt, then decompose and vaporize, leaving a void in the substrate. By this means, the moving laser beam driven by stepper motors is able to cut structures such as microchannels and wells on the substrate. The cross section of the microchannel mainly depends on the shape of the laser beam, its scanning speed, the laser power and the thermal diffusivity of substrate material. The energy of the laser beam has a Gaussian distribution, resulting in a Gaussian shaped cross section. Figure 2 shows the SEM micrograph of the cross section of the microchannel engraved in **PMMA** substrate. The microfluidic structure was designed to have a microchannel width of 100 μm. The microchannel, which was engraved at a laser power of 0.75 W and a beam speed of 32 mm s^{-1}, was measured to be 100 μm wide and 75 μm deep.

Besides the shape of the laser beam, we also investigated the effects of the laser power and the beam speed on microchannel dimensions. The relationship between the laser power and the channel dimensions is illustrated in figure 3(*a*). The beam speed was fixed at 25.6 mm s^{-1}, i.e., 4% of the maximum speed, while the laser power was varied from 0.75 W to 2.625 W. It can be seen that the microchannel depths increased linearly with the laser power, from 50 μm to 450 μm, while the microchannel width slightly increased from 150 μm to 250 μm. The findings are in line with the results observed by Klank *et al* [7, 21]. Figure 3(*b*) shows the dependence of microchannel dimensions on the laser beam speed. The laser power was kept at a constant value of 1.75W, i.e., 7% of the maximum power, while the beam speed was varied from 5.12 mm s^{-1} to 7.04 mm s^{-1}. It is observed that with the increase of the beam speed, the microchannel depth decreased significantly from 1500 μm to 150 μm, while the microchannel width dropped slightly, from 400 μm to 200 μm. The result suggests that the microchannel widths and depths were inversely proportional to the beam speed. This is due to the fact that when the laser beam moves at a higher speed, it spends shorter time at each spot, and consequently less heat is absorbed by the material, resulting in a shallower and narrower microchannel.

The above discussion shows that **PMMA** microfluidic devices can be easily produced by CO_2 laser micromachining. The dimensions of microstructures could be precisely controlled by adjusting parameters such as the laser power and the scanning speed. With rapid 'idea-to-prototype' turnaround time of a few hours, CO_2-laser micromachining is particularly suitable for scientific trials and small-scale production.

3.2. Thermal bonding

To develop an effective thermal bonding method, thermal properties of **PMMA** were intensively studied. **PMMA** consists of chains of methacrylate monomers via the covalent bond between the molecules, serving as the backbone in the polymer. There are three important types of bonds within the polymer chains, formed by different reactions during radical polymerization, namely regular polymer backbone bonds, unsaturated end groups and head-to-head bonds. Figure 4 shows the reaction steps for the formation of these three groups [22]. The polymer chain propagation consists of the addition of one monomer unit to the growing macroradical, in general by a 'head-to-tail' mechanism. This means that, stereochemically, the monomer is always bound to the polymer chain by its least substituted carbon. This 'head-to-tail' propagation leads to a uniform backbone with C–C bonds that are thermally stable up to 300 °C. Above this, they break up statistically, known as random chain scission. The unsaturated end groups and the head-to-head bonds are formed mainly by termination reactions. Apart from termination by other radical species, two active polymer chains can also terminate themselves in two differentways: either by disproportionation, leading to a double bond in one chains end group (thermally stable up to 250 °C), or by head-to-head coupling. In the latter case, a thermally very unstable C–C bond is formed, which breaks easily at temperatures as low as 180 °C. Depending on the thermal bond stability, the polymer chain is activated by bond scission at the corresponding temperature and is completely depolymerized by an unzipping reaction. Unzipping is a depolymerization reaction, where the polymer chain fragments into its constituent

monomer units. According to Nising *et al* [22], when **PMMA** is heated, it degrades back into monomer in three different steps:

- At about 180 °C, the head-to-head coupling breaks.
- At around 250 °C, unsaturated end groups start to unzip.
- At above 300 °C, random chain scission appears, the structure is quickly damaged.

Corresponding to this temperature behavior, **PMMA** does not degrade gradually but step by step. Although **PMMA** starts to soften at the glass transition point (about 105 °C), it will not massively depolymerize until 180 °C. We found that the structural integrity can still be warranted at a temperature slightly below 180 °C by exerting a relatively low bonding pressure. All previous thermal bonding methods tried to keep the temperature just above the glass transition temperature to protect pre-fabricated microstructures [17]; however, a higher temperature can offer better bonding, because more bonds are broken during bonding and reconnected after cooling. Therefore, in our process, a high temperature of 165 °C and low bonding pressure of less than 20 kPa were applied. The experimental implementation of this bonding technique was described in the microfabrication section. Our bonding pressure is much lower compared to Alonso-Amigo's work [17], where a pressure of 7-14 MPa was applied to attain efficient bonding at the glass transition temperature of 105 °C.

The bonding strength between two **PMMA** substrates was investigated as described in the section 2. Four out of the six specimens experienced bonding failure, while the other two broke at the edge of the bonding area. The average break force for the four specimens was 645 N, corresponding to a bond failure pressure of 2.15 MPa, while the maximum bonding strength reported in the literature was about 1MPa for bonding at glass transition temperature [23]. Devices formed by our thermal bonding approach are thus much stronger and the same chip can be used for several CE experiments.

Figure 5 shows the cross section of several bonded microchannels. The microchannels were fabricated by different laser powers as described previously. After cutting and polishing, images of

the cross sections were taken by the SEM. Almost no signs of the bonding interface were observed. Despite the high bonding temperature, all the microchannels retain their original Gaussian shapes. The channel dimensions before and after bonding are listed in table 3. The maximum deviations are 1.5% and 1.8% for the channel width and depth, respectively. The results show that the new bonding technique is very promising.

3.3. Electroosmotic mobility

EOF is generated by the surface charge on the microchannel walls in combination with an electric field along the microchannel. Typically polymers have lower surface charge density compared to glass. Electroosmotic velocity of 930 μm s^{-1} in the fabricated **PMMA** microchannel was obtained by the current monitoring method. The electroosmotic mobility of the laser-ablated **PMMA** substrate was calculated to be 2.47 $\times$ 10^{-4} cm^2 V^{-1} s^{-1}. This is comparable with the electroosmotic mobility of the native atmospheric molded **PMMA** microchannel (2.37 $\times$ 10^{-4} cm^2 V^{-1} s^{-1}) [20], while the value is much smaller than the electroosmotic mobility of the glass microchips, which was reported to be 4.46 $\times$ 10^{-4} cm^2 V^{-1} s^{-1} [20]. Normally the electrophoretic velocities of negatively charged compounds will be greater than the EOF generated by the CO_2 laser ablated **PMMA** device, causing the net velocity from the cathodic to the anodic reservoir. Hence, in most cases, reverse polarity was used for CE separation.

3.4. Microchip CE

As further evidence of the utility of microdevices bonded by the new method, we performed electrophoretic separation of $\phi X174$-*Hae III* dsDNA digest and a mixture of fluorescein and carboxyfluorescein.

3.4.1. Free solution electrophoresis.

Figure 6 depicts the electropherogram of the separation of fluorescein and carboxyfluorescein. The two chemicals were separated in just over 40 s, with a resolution of 1.72. The migration times for carboxyfluorescein and fluorescein were 25 s and 41 s, respectively, and the half-peak widths were 2.8 s and 3.7 s, respectively. The experiment was repeated three times and the standard deviations for migration time and half-peak width were less than 0.5% and 5%, respectively. Compared with the CE reported in the literature using **PMMA** chips fabricated by other methods [10], our result was comparable or superior to them in terms of speed and resolution. This could be due to the microchannel profile. The Gaussian-shaped microchannel attained from CO_2 laser has smaller cross section than square or circular channels. As a result, Joule heat can be dissipated more effectively and better performance can be achieved.

3.4.2. Separation of DNA fragments.

The capability of the microfabricated plastic chip for electrophoretic separation was also tested by the separation of DNA fragments. Figure 7 shows the electropherogram of ϕ*X*174-*Hae III* dsDNA digest separated using an electric field strength of 300 V cm^{-1}. The result was repeated three times, and the relative standard deviations were less than 0.8% and 5% for migration time and half peak width, respectively. As seen from the electropherogram, all of the 11 fragments were clearly separated and baseline resolution for the 271/281 base pair fragments was achieved. The results indicate that efficient electrophoretic separation of DNA fragments can be obtained using the microchip fabricated by this novel high-temperature, low-pressure technique. Our results were comparable to works that employ **PMMA** microchannels fabricated by injection molding and adhesive bonding technique [1].

4 Conclusions

In this paper, a novel thermal direct bonding technique for **PMMA** was developed and successfully implemented. CO_2 laser micromachining was used to fabricate **PMMA** microchannels.

Microchannel depths from 50 μm to 1500 μm and widths from 150 μm to 400 μm were achieved by adjusting the laser power and scanning speed. Instead of the conventional low-temperature/high-pressure approach, we used high temperature of 165 °C and low pressure of less than 20kPa to keep the structural integrity of microstructures on **PMMA**. The measured bonding strength was as high as 2.15 MPa. Examination of cross sections of the microchannels validates the good bonding quality. Electroosmotic mobility of laser-ablated microchannel was 2.47×10^{-4} cm^2 V^{-1} s^{-1}. Rapid and efficient electrophoretic separations of ϕ*X*174-*Hae III* dsDNA digest and a mixture of fluorescein and carboxyfluorescein were successfully carried out on our fabricated microdevices. This new methodology for generation of microfluidic structures should facilitate the rapid fabrication of microdevices at low cost, and it could be widely used in biological, clinical and forensic applications.

Acknowledgments

The authors would like to thank the Ministry of Education of Singapore for financial support of this work (contract number RG11/02) as well as Dr Wu Zhigang for his initial work on this project. Sun Yi would also like to thank the National Institute of Education for providing the research scholarship.

References

[1] Dang F, Shinohara S, Tabata O, Yamaoka Y, Kurokawa M, Shinohara Y, Ishikawa M and Baba Y 2005 Replica multichannel polymer chips with a network of sacrificial channels sealed by adhesive printing method *Lab. Chip* **5** 472–8

[2] Shadpour H, Musyimi H, Chen J F and Soper S A 2006 Physiochemical properties of various polymer substrates and their effects on microchip electrophoresis performance *J. Chromatogr.* A **1111** 238–51

[3] Kricka L J, Fortina P, Panaro N J, Wilding P, Amigo G A and Becker H 2002 Fabrication of plastic microchips by hot embossing *Lab. Chip* **2** 1–4

[4] Wainright A, Nguyen U T, Bjornson T and Boone T D 2003 Preconcentration and separation of double-stranded DNA fragments by electrophoresis in plastic microfluidic devices *Electrophoresis* **24** 3784–92

[5] Madou M 1997 *Fundamentals of Microfabrication* (Boca Raton, FL: CRC Press LLC)

[6] Roberts M A, Rossier J S, Bercier P and Girault H 1997 UV laser machined polymer substrates for the development of microdiagnostic systems *Anal. Chem.* **96** 2035–42

[7] Klank H, Kutter J P and Geschke O 2002 CO2-laser micromachining and back-end processing for rapid production of **PMMA**-based microfluidic system *Lab. Chip* **2** 242–6

[8] Weigl B H 2001 Design and rapid prototyping of thin-film laminate-based microfluidic devices *Biomed. Micro Devices* **3** 267–74

[9] Martynova L, Locascio L E, Gaitan M, Kramer G W, Christensen R G and MacCrehan W A 1997 Fabrication of plastic microfluid channels by imprinting methods *Anal. Chem.* **69** 4783–9

[10] Kelly R T and Woolley A T 2003 Thermal bonding of polymeric capillary electrophoresis microdevices in water *Anal. Chem.* **75** 1941–5

[11] Ford S M, Davies J, Kar B, Qi S D, McWhorter S, Soper S A and Malek C K 1999 High-aspect ratio micromachining in polymethylmethacrylate (**PMMA**) using x-ray lithography for the fabrication of micro-electrophoresis devices *J. Biomech. Eng.* **121** 13

[12] Yussuf A A, Sbarski I, Hayes J P, Solomon M and Tran N 2005 Microwave welding of polymeric-microfluidic devices *J. Micromech. Microeng.* **15** 1692–9

[13] Brown L, Koerner T, Horton J H and Oleschuk R D 2006 Fabrication and characterization of poly(methylmethacrylate) microfluidic devices bonded using surface modifications and solvents. *Lab*. *Chip* **6** 66–73

[14] McCormick R M, Nelson R J, AlonsoAmigo M G, Benvegnu F and Hooper H H 1997 Microchannel electrophoretic separations of DNA in injection-molded plastic substrates *Anal*. *Chem*. **69** 2626–30

[15] Bianchi F, Wagner F, Hoffmann P and Girault H H 2001 Electroosmotic flow in composite microchannels and implications in microcapillary electrophoresis systems *Anal*. *Chem*. **73** 829–36

[16] Liu Y, Fanguy J C, Bledsoe J M and Henry C S 2000 Dynamic coating using polyelectrolyte multilayers for chemical control of electroosmotic flow in capillary electrophoresis microchips *Anal*. *Chem*. **72** 5939–44

[17] Alonso-Amigo M G and Adams T 2003 Development of a plastic microfluidics chip *IVD Technol*. **3** 41–5

[18] Liu Y J, Ganser D, Schneider A, Liu R H, Grodzinski P and Kroutchinina N 2001 Microfabricated polycarbonate CE devices for DNA analysis *Anal*. *Chem*. **73** 4196–201

[19] Wabuyele M B, Ford S M, Stryjewaski W, Barrow J and Soper S A 2001 Single molecule detection of double-stranded DNA in poly(methylmethacrylate) and polycarbonate microfluidic devices *Electrophoresis* **22** 3939–48

[20] Wang J, Muck A, Chatrathi M P, Chen G, Mittal N, Spillman S D and Obeidat S 2005 Bulk modification of polymeric microfluidic devices *Lab*. *Chip* **5** 226–30

[21] Snakenborg D, Klank H and Kutter J P 2004 Microstructure fabrication with a CO2 laser system *J. Micromech. Microeng*. **14** 182–9

[22] Nising P, Zeilmann T and Meyer T 2003 On the degradation and stabilization of Poly(Methyl Methacrylate) in a continuous process *Chem*. *Eng*. *Technol*. **26** 599–604

[23] Sung W C, Lee G B, Tzeng C C and Chen S H 2001 Plastic microchip electrophoresis for genetic screening: Theanalysis of polymerase chain reactions products of fragile X (CGG)n alleles *Electrophoresis* **22** 1188–93

List of Tables

List of Figures

No	Step	Temperature (°C)	Time (min)
1	Heating	From 25 to 165	10
2	Bonding	165	30
3	Cooling	From 165 to 80	20
4	Annealing	80	30
5	Cooling	From 80 to 25	30

Table 1.

Step	Time (s)	Voltages (V)				Electric field (V cm^{-1})
		A[a]	B	C	D	
Injection	20	Float	0	700	Float	350
Separation	150	0	Float	Float	4000	500

Table 2.

	Before bonding		After bonding	
Laser power (W)	Channel width (μm)	Channel depth (μm)	Channel width (μm)	Channel depth (μm)
0.75	126.6	37.1	128.5	36.4
1.37	199.9	123.5	200.4	121.2
1.5	208.1	180.2	208.5	180.9
1.625	214.7	228.3	215.2	225.4
1.75	221.5	275.3	221.9	270.8
1.875	227.8	338.2	228.6	331.9

Table 3.

Unit: cm

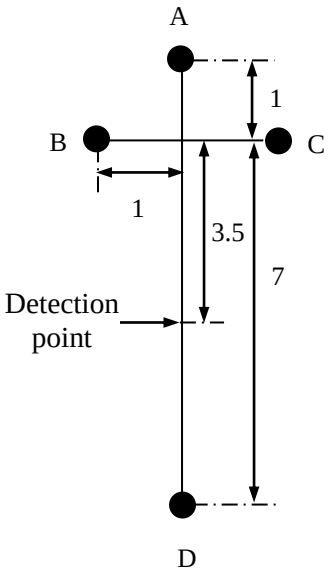

Fig. 1

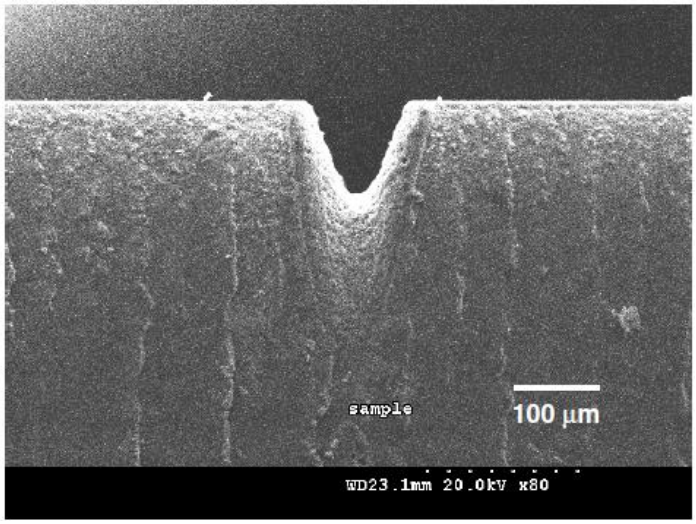

Fig. 2

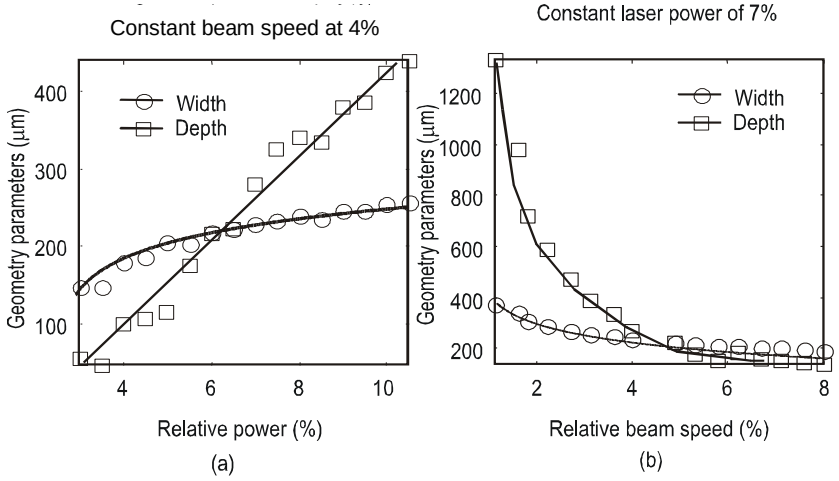
Constant beam speed at 4%
Width
Depth
Geometry parameters (μm)
400
300
200
100
4
6
8
10
Relative power (%)
(a)
Constant laser power of 7%
Width
Depth
Geometry parameters (μm)
1200
1000
800
600
400
200
2
4
6
8
Relative beam speed (%)
(b)

Fig. 3

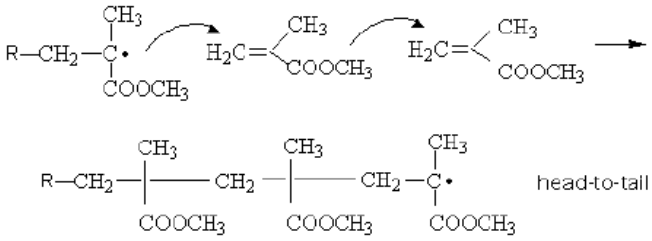

Addition of monomer molecules to chain (anti-Markownikoff)

Termination reaction

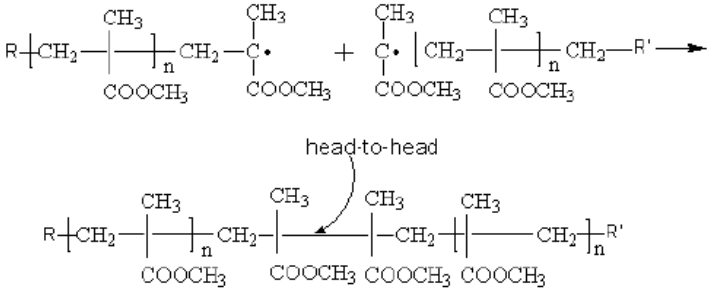

Termination by forming a head-to-head bond

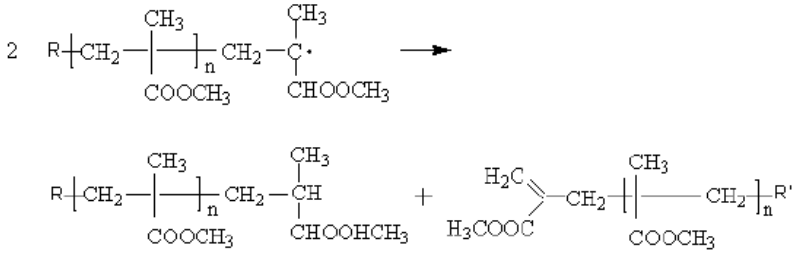

Termination by disproportionation, leading to an unsaturated end group

Fig. 4

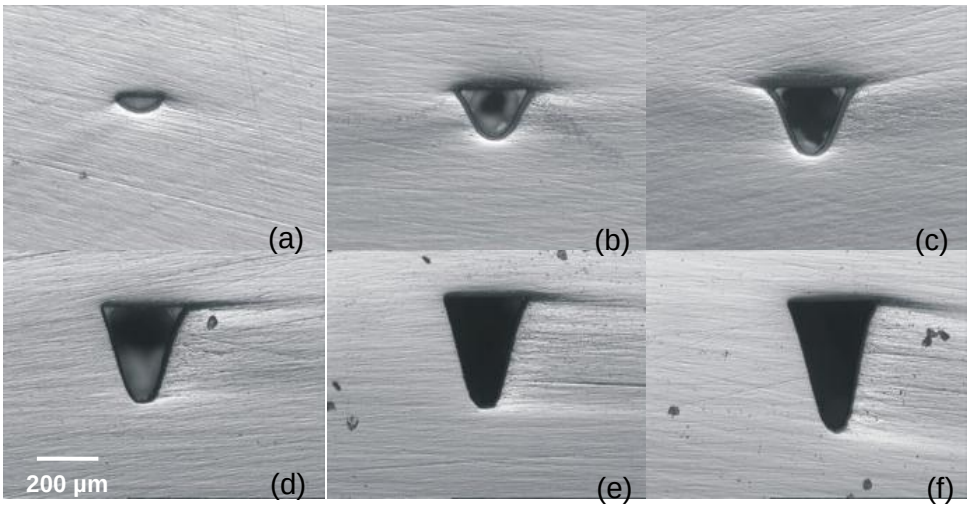

Fig. 5

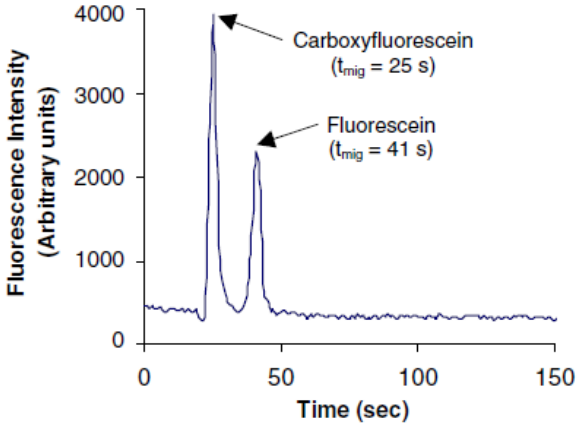
4000
3000
2000
1000
0
Fluorescence Intensity
(Arbitrary units)
Carboxyfluorescein
(t_{mig} = 25 s)
Fluorescein
(t_{mig} = 41 s)
0
50
100
150
Time (sec)

Fig. 6

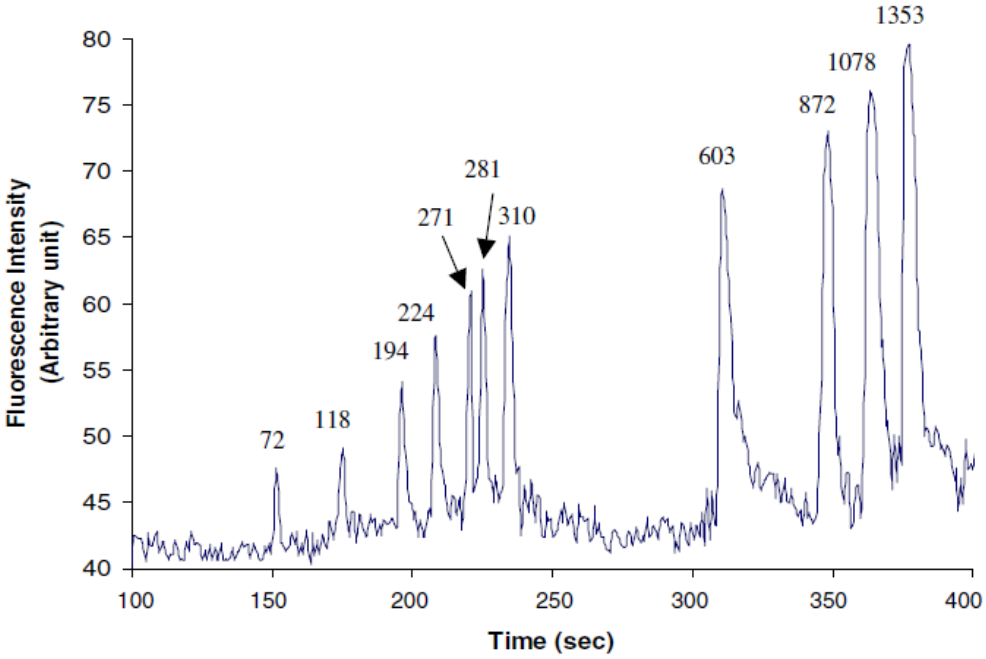
Fluorescence Intensity
(Arbitrary unit)
Time (sec)
80
75
70
65
60
55
50
45
40
100
150
200
250
300
350
400
72
118
194
224
271
281
310
603
872
1078
1353

Fig. 7